



**Ferromagnetic resonance and damping properties of CoFeB thin films as free layers in MgO-based magnetic tunnel junctions**

Xiaoyong Liu, Wenzhe Zhang, Matthew J. Carter, and Gang Xiao

Citation: [Journal of Applied Physics](#) **110**, 033910 (2011); doi: 10.1063/1.3615961

View online: <http://dx.doi.org/10.1063/1.3615961>

View Table of Contents: <http://scitation.aip.org/content/aip/journal/jap/110/3?ver=pdfcov>

Published by the [AIP Publishing](#)

---

**Advertisement:**



**Re-register for Table of Content Alerts**

Create a profile.



Sign up today!



# Ferromagnetic resonance and damping properties of CoFeB thin films as free layers in MgO-based magnetic tunnel junctions

Xiaoyong Liu,<sup>1,a)</sup> Wenzhe Zhang,<sup>2</sup> Matthew J. Carter,<sup>3</sup> and Gang Xiao<sup>2</sup>

<sup>1</sup>National Institute of Standards and Technology, Gaithersburg, Maryland 20899, USA

<sup>2</sup>Physics Department, Brown University, Providence, Rhode Island 02912, USA

<sup>3</sup>Micro Magnetics, Inc., Fall River, Massachusetts 02720, USA

(Received 1 March 2011; accepted 24 June 2011; published online 8 August 2011)

We have investigated the magnetization dynamics of sputtered  $\text{Co}_{40}\text{Fe}_{40}\text{B}_{20}$  thin films in a wide range of thicknesses used as free layers in MgO-based magnetic tunnel junctions, with the technique of broadband ferromagnetic resonance (FMR). We have observed a large interface-induced magnetic perpendicular anisotropy in the thin film limit. The out-of-plane angular dependence of the FMR measurement revealed the contributions of two different damping mechanisms in thick and thin film limits. In thinner films ( $< 2$  nm), two-magnon scattering and inhomogeneous broadening are significant for the FMR linewidth, while the Gilbert damping dominates the linewidth in thicker films ( $\geq 4$  nm). Lastly, we have observed an inverse scaling of Gilbert damping constant with film thickness, and an intrinsic damping constant of 0.004 in the CoFeB alloy film is determined. © 2011 American Institute of Physics. [doi:10.1063/1.3615961]

## I. INTRODUCTION

Magnetic tunnel junctions (MTJs) have been extensively investigated for basic understanding of spin-dependent phenomena and applications to magnetic random access memory (MRAM), read heads in hard disk drives, as well as spin-logic based devices.<sup>1-4</sup> Extremely large tunneling magnetoresistance (TMR) at room temperature has been predicted and demonstrated in MTJs using (001)-textured MgO as a tunnel barrier.<sup>5-8</sup> The ferromagnetic alloy, CoFeB in certain composition, is the preferred magnetic free-layer (FL) electrode material in the MgO-based MTJs, because of the highest TMR value attainable. CoFeB thin films can grow smoothly on MgO barrier with minimal roughness. Furthermore, a near-epitaxial relationship between MgO and CoFeB can be achieved with proper post-deposition thermal annealing.

Apart from high TMR values, it is also important to understand the magnetic dynamics and to be able to tune the damping properties of CoFeB, for realizing high speed spintronic devices. For instance, the damping constant of a FL determines the critical switching current in a spin-torque-transfer (STT) based device.<sup>9,10</sup> Small damping values are essential in minimizing power consumption in STT based MRAM. For TMR read heads, the thermal magnetic noise is proportional to the damping constant of the FL, which affects the signal-to-noise ratio of a read head.<sup>11</sup> On the other hand, to improve thermal stability,<sup>12</sup> a large damping constant is preferred in all metallic current-perpendicular-to-plane giant-magnetoresistance (CPP GMR) read sensors.

Ferromagnetic resonance (FMR) is a versatile technique and is widely used for studying magnetic anisotropy and relaxation in thin films and multi-layers. There have been several reports<sup>13-18</sup> on the dynamic properties of CoFeB thin

films, but few discussions on the damping mechanism are made. Especially lacking is the FMR study on realistic CoFeB thin films used as FLs in MgO based MTJs. The environment provided by the MTJ stacks cannot be decoupled from the dynamical properties of the FLs. In this work, we present a broadband FMR study particularly for the CoFeB FLs used in MgO based MTJs. We will show the evolution of damping property and linewidth broadening as we vary the thickness of the CoFeB films in a wide range. As a result of our work, we have uncovered both the intrinsic and extrinsic dynamical properties of the CoFeB FLs.

## II. EXPERIMENTAL DETAILS

Multiple samples of CoFeB free layer (FL) with the structure (thicknesses in nanometers) of MgO(2)/ $\text{Co}_{40}\text{Fe}_{40}\text{B}_{20}$  ( $t = 1-20$ )/Ta(5)/Ru(10) were deposited onto a thermally oxidized Si wafer under ambient temperature using magnetron sputtering with a base vacuum of  $\approx 2 \times 10^{-6}$  Pa. To best mimic the condition used in TMR fabrication process, prior to experiment, all samples were annealed at 310° C for 4 h in high vacuum with an applied field of 4.5 kOe (357 kA/m) in the film plane to crystallize initially amorphous CoFeB into a bcc(001) textured structure as well as setting an easy axis for films. In addition, a series of MTJ reference samples with the exact same free layer structure (Full stack: Ta(5)/Ru(30)/Ta(5)/ $\text{Co}_{50}\text{Fe}_{50}$ (3)/IrMn(18)/ $\text{Co}_{50}\text{Fe}_{50}$ (3)/Ru(0.9)/ $\text{Co}_{40}\text{Fe}_{40}\text{B}_{20}$ (3)/MgO(2)/FL) were deposited and examined using current-in-plane-transport (CIPT) technique.<sup>19</sup> TMR values are found to increase gradually with FL thickness, from 150% for 1 nm FL to about 200% for 20 nm FL as shown in Fig. 1. The high TMR values over a broad thickness range of FL imply the good epitaxial texture of CoFeB films and small interfacial roughness between CoFeB/MgO. FMR spectra were taken at National Institute of Standards and Technology (NIST) Gaithersburg campus using a broadband coplanar waveguide

<sup>a)</sup>Electronic mail: xiaoyong.liu@nist.gov.

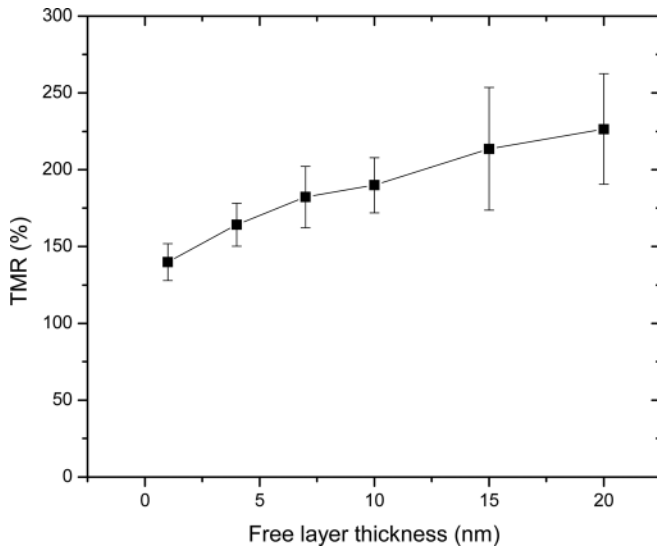


FIG. 1. TMR as a function of CoFeB FL thickness for the reference MTJ samples. Error bar denotes the fitting uncertainties during each CIPT measurements.

as a function of sweeping field for a set of microwave frequencies (3 to 30 GHz) with applied field parallel and perpendicular to the film plane. Field modulation and lock-in techniques were used to obtain conventional field derivative of the sample absorption. The resonance signals were found to be Lorentzian-like at all frequencies. Fitting of signals gives the resonant field ( $H_{res}$ ) and the peak-to-peak linewidth ( $\Delta H$ ). In order to investigate the linewidth broadening mechanism, we measured the angular dependence of FMR spectra by varying applied field from in-plane ( $\theta_h = 0^\circ$ ) to out-of-plane ( $\theta_h = 90^\circ$ ) for a fixed frequency. Sample alignment is performed by recording resonant field as a function of sample stage angle with a  $15^\circ$  span near in-plane at  $1^\circ$  intervals. The stage position where the minimal resonant field is obtained is defined as “in-plane”.

### III. RESULTS AND DISCUSSION

We first present data taken at in-plane configuration. Figure 2(a) shows the frequency dependence of resonant field in our samples with the magnetic field applied in sample plane. The CoFeB film properties for each thickness were determined by fitting  $H_{res}$  versus frequency curve to Kittel formula  $f^2 = \left(\frac{\mu_0 \gamma}{2\pi}\right)^2 H(H + M_{eff})$  using  $M_{eff}$  and gyromagnetic ratio  $\gamma$  as fitting parameters, assuming negligible contributions from in-plane anisotropy field  $H_k$  ( $H_k$  is normally about 20 Oe) and in-plane demagnetization factor (sample size is around 5 mm). The fitted  $\gamma$  value is found to be a constant of  $29.0 \pm 0.3$  GHz/T across different samples. The effective magnetization is defined as  $M_{eff} = M_S - H_K^\perp$ , where  $M_S$  is the saturation magnetization and  $H_K^\perp$  is the perpendicular anisotropy field. Figure 2(b) plots out the extracted effective magnetization  $M_{eff}$  against film thickness. It can be seen that  $M_{eff}$  can be fitted linearly to the inverse of CoFeB film thickness. The constant and the slope represent the bulk and surface contributions to anisotropy, respectively. From Fig. 2(b), the bulk saturation field  $M_S$  is extracted to be about 1.8 T. Separate vibrating sample magnetometry (VSM) mea-

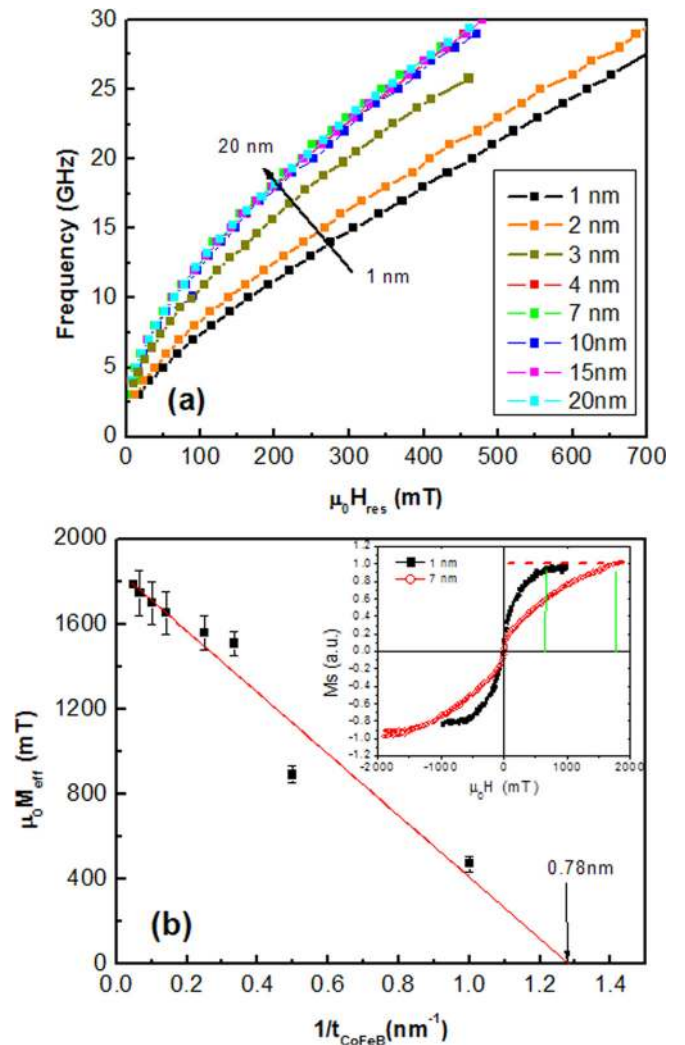


FIG. 2. (Color online) (a) Field dependence of resonance frequency for CoFeB films with different thicknesses. (b) Effective magnetization as a function of  $1/t_{CoFeB}$ . The arrow denotes the critical thickness below which the magnetic easy axis to be out-of-plane. Inset: Out-of-plane hysteresis curves for samples with 1 nm (filled) and 7 nm (open), respectively.

surement reveals that saturation magnetization of CoFeB is about 1.7 T, and remains constant within the thickness range of our films. Perpendicular surface anisotropy constant is found to be  $K_s = 1.03 \pm 0.02$  mJ/m<sup>2</sup> (1.03 erg/cm<sup>2</sup>). This number is slightly smaller than to what was reported in a similar structure (1.3 mJ/m<sup>2</sup> and 1.8 mJ/m<sup>2</sup>, respectively).<sup>14,15</sup> Furthermore, it is noticed that  $M_{eff}$  decreases to zero at around  $t = 0.78 \pm 0.02$  nm, below which the surface anisotropy will overcome demagnetization field and cause the magnetic easy axis to be out-of-plane. This is also confirmed by direct VSM measurements with field applied out-of plane. The inset of Fig. 2(b) shows the magnetization as a function of out-of-plane field for 7 nm and 1 nm thick samples. For the thicker sample, a large field of 1.7 T is required to saturate the magnetization, whereas for the thinner sample, only 0.5 T is required. Such reduced saturation field is the indication of induced perpendicular anisotropy.

Our result is consistent with recent reports<sup>14,15</sup> that a perpendicular MTJ device was realized when the CoFeB free layer thickness (with proper capping layer) was reduced to

the thin film limit. The origin of induced perpendicular surface anisotropy is not well understood and is initially believed to be related to hybridization of Fe  $3d$  and O  $2p$  orbitals at Fe/MgO interface. It was found out later that Ta/CoFeB interface also makes a key contribution.<sup>15</sup> The critical thickness to observe full perpendicular anisotropy from our sample (0.78 nm) is found to be smaller than what is reported in Refs.<sup>14,15</sup> (1 nm to 1.5 nm). The relatively smaller  $K_s$  value in our samples may be responsible for this difference. CoFeB is indeed an excellent FL material, not only for the high TMR value attainable in the MgO based MTJs, but also for its versatility in creating in-plane and out-of-plane easy axis upon a variation of thickness.

Next, we focus on the dynamical properties of CoFeB as a FL. We have measured the in-plane linewidth ( $\Delta H$ ) as a function of FMR frequency ( $f$ ) for various CoFeB thicknesses, as shown in Fig. 3(a). A clear increase in  $\Delta H$  is observed upon reducing thickness. For samples thicker than 2 nm,  $\Delta H$  increases linearly with  $f$  over the entire experimental frequency range. However, for samples with thickness equal to or thinner than 2 nm,  $\Delta H$  becomes increasingly nonlinear with  $f$  at higher frequencies. Such a nonlinear behavior is related to two-magnon scattering, which comes from coupling between the uniform FMR mode and the degenerate spin waves, leading to an additional magnetic relaxation channel.<sup>20</sup> Our data suggests that two-magnon scattering is increasingly significant as the CoFeB thickness is reduced, particularly, below 2 nm. Therefore, if used as in a perpendicular MTJ, the two-magnon scatterings in the thin CoFeB FL will play an important role in the dynamics at high frequencies.

It is known<sup>21</sup> that the dispersion relation for spin-waves will have a positive initial slope when a field is applied perpendicularly to the film plane. The FMR frequency falls to the bottom of the energy band and, therefore, there are no magnons degenerates with the uniform procession. Consequently, in the perpendicular configuration, two-magnon scattering is suppressed. In Fig. 3(b), we present  $\Delta H$  versus  $f$  data measured with the applied field perpendicular to the

films for 1 nm and 2 nm samples. Clear linear dependence on frequency is observed for both samples, except some deviations from linearity at low frequency ranges, which results from insufficient field to fully saturate the magnetization. More importantly, when compared to the in-plane linewidths for the same samples at the same frequencies (Fig. 3(a)), these perpendicular linewidths are smaller, confirming the absence of two-magnon scattering. It is also noticed that inhomogeneous broadening  $\Delta H_0$  (defined as zero-frequency-intercept of linewidth) increases with reducing thickness. This may be related to anisotropy dispersion. Such dispersion is thickness dependent and accounts for a large contribution to the damping below 2 nm.

In order to further understand the linewidth broadening mechanism, we measured FMR spectra by varying the angle  $\theta_h$  between the applied field and film plane. Figure 4 shows the dependence of  $\Delta H$  on  $\theta_h$  for CoFeB films with thicknesses of 1 nm and 4 nm, at a fixed frequency of 10 GHz and 7 GHz, respectively. For the 1 nm sample (Fig. 4(a)),  $\Delta H$  slowly increases as the external field tips out of sample plane, reaching a peak at around  $\theta_h = 70^\circ$ , but then quickly decreases to a minimum in the perpendicular configuration ( $\theta_h = 90^\circ$ ). The significant increase of  $\Delta H$  at intermediate angle is related to the magnetic dragging effect, where magnetization is not parallel to, but instead lags behind the external field direction due to demagnetization field. The linewidth ( $\mu\Delta H = 8$  mT) in perpendicular configuration is smaller than that in the parallel configuration ( $\mu\Delta H = 11$  mT) because of the absence of two-magnon scattering, which is consistent with data from Fig. 3. For the 4 nm film (Fig. 4(b)), however,  $\Delta H$  increases monotonically with field angle, reaching a maximum at  $\theta_h = 90^\circ$ . Such a peak of  $\Delta H$  at  $\theta_h = 90^\circ$  is an experimental artifact due to a combination effect of large  $M_{eff}$  for our thicker samples and probable small misalignment of the sample stage at  $90^\circ$ .

The measured resonance linewidth consists of Gilbert damping ( $\Delta H_{in}$ ), two magnon scattering ( $\Delta H_{2m}$ ), and an inhomogeneous broadening ( $\Delta H_0$ ). Gilbert damping is a

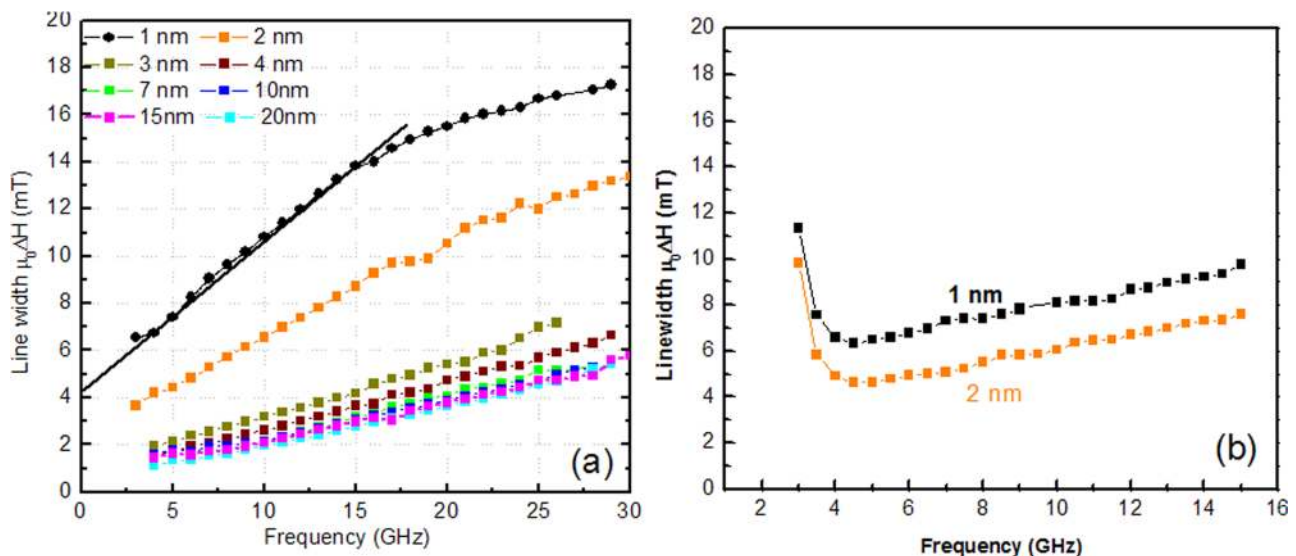


FIG. 3. (Color online) Dependence of FMR linewidth  $\Delta H$  on frequency obtained in (a) parallel and (b) perpendicular configurations for different CoFeB thicknesses.

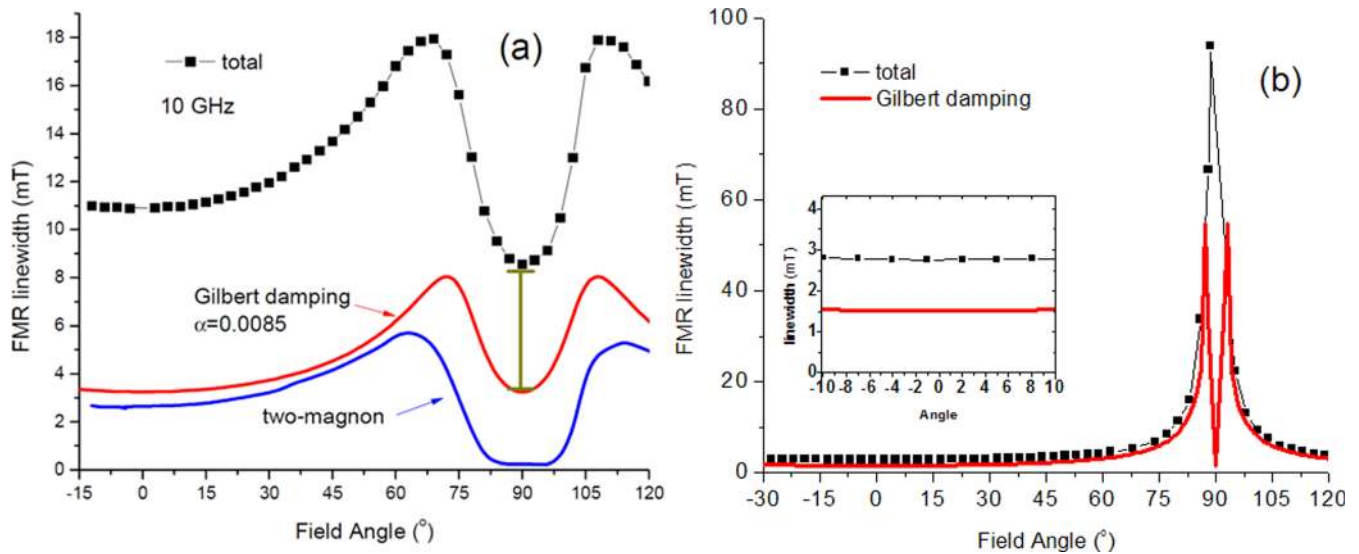


FIG. 4. (Color online) Angular dependence of  $\Delta H$  for samples with thickness of (a) 1 nm and (b) 4 nm, respectively. Square lines indicate the experimental data. Solid lines show two components of total  $\Delta H$ , which are due to Gilbert damping, and two-magnon scattering, respectively. The vertical bar at  $\Delta H = 90^\circ$  in (a) denotes the contribution from an angle-independent inhomogeneous broadening term. The inset in (b) is an enlarged view in the vicinity of  $\Delta H = 0^\circ$ . The parameters used for the calculations are shown in the figure. The peak at  $90^\circ$  in (b) is due to misalignment.

measure of the microscopic mechanism by which the absorbed microwave energy is dissipated from the spin system to the lattice, and it is proportional to frequency, i.e.,  $\Delta H_{in} = 4\pi f \alpha / \sqrt{3} \gamma \Xi$ . Where  $\alpha$  is the Gilbert damping constant, and  $\Xi$  is a numerically calculable function of the external applied field  $H$ , the effective magnetization  $M_{eff}$ , and the magnetization direction  $\theta_m$ , provided  $\alpha$  is known from frequency dependence of linewidth.<sup>22</sup> With the knowledge of  $\Delta H_{in}$  and  $\Delta H_0$ , angular dependence of two-magnon scattering contributions can then be separated from total measured linewidth as shown in the solid blue lines in Fig. 4(a). Clearly a broad valley centered around  $\theta_h = 90^\circ$  is observed for  $\Delta H_{2m}$ , which is a reflection of the critical angle for  $\theta_h$ , above which two-magnon scattering contribution is suppressed. Our result is consistent with prior demonstrations<sup>20</sup> that as long as magnetization angle  $\theta_m$  relative to film plane is less than  $\pi/4$  (equivalent to  $\theta_h = 72^\circ$  in our system), the degeneracy of finite spin wave vector and FMR mode, and hence two-magnon contribution to linewidth, always exist. It is apparent from Fig. 4(a) that inhomogeneous broadening (including both  $\Delta H_{2m}$  and  $\Delta H_0$ ) exhibits significant contributions for 1 nm thick film: At  $\theta_h = 90^\circ$ ,  $\Delta H_0$  (vertical bar) contributes about 50% of the total linewidth, and at  $\theta_h = 0^\circ$ , the Gilbert damping, inhomogeneous broadening and two-magnon damping all contribute comparably to the linewidth. While for 4 nm sample, our data shows that Gilbert damping is the dominant source, and its angular dependence follows that of total linewidth quite well when away from  $\theta_h = 90^\circ$  (Fig. 4(b)). Enlarged view near  $\theta_h = 0^\circ$  region indicates a small constant offset of about 1.2 mT. This offset is the same as that zero-frequency offset ( $\Delta H_0$ ) from in-plane data.

We now turn to the thickness dependence of Gilbert damping constant  $\alpha$  for CoFeB films as shown in Fig. 5. Because of various extrinsic contributions to linewidth for films with different thicknesses, we evaluated  $\alpha$  directly from the linear fit of  $\Delta H$  versus  $f$  in perpendicular configuration for

films with  $t \leq 2$  nm. While for thicker films ( $t > 2$  nm),  $\alpha$  was obtained from in-plane data due to the negligible contributions from  $\Delta H_{2M}$  and  $\Delta H_0$ . The  $\alpha$  value roughly follows  $1/t_{\text{CoFeB}}$  in a linear fashion, decreasing from above 0.008 with  $t_{\text{CoFeB}} = 1$  nm to about 0.004 with  $t = 10$  nm, and saturating with a further increase of thickness. Such finite size effect in damping (enhancement of  $\alpha$  at thinner films) cannot be due to surface roughness induced two-magnon scattering, whose effect has been analyzed and removed by taking out-of-plane measurement. Mizukami *et al.*<sup>23</sup> attributed the damping increase in his Ta/Ni<sub>80</sub>Fe<sub>20</sub>/Ta structure to the reduction of saturation magnetization  $M_S$  with Ni<sub>80</sub>Fe<sub>20</sub> thickness. This argument does not support our data since VSM data shows that  $M_S$  is constant over the thickness range of our samples within experimental uncertainty. The increase of damping value using Ta capped

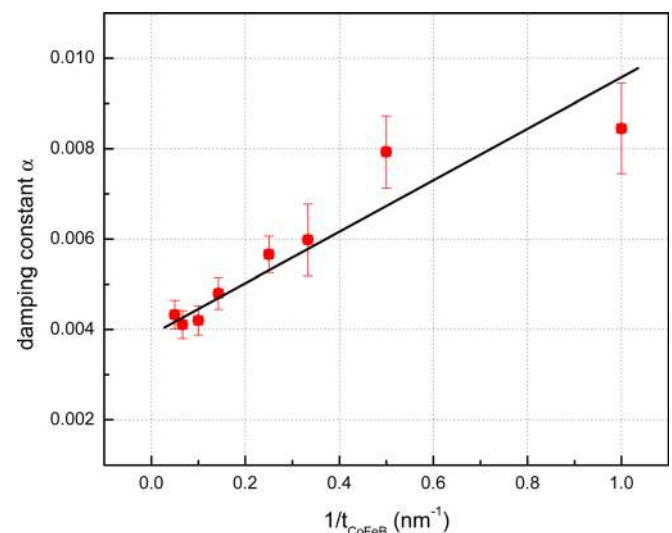


FIG. 5. (Color online) The plot of Gilbert damping constant  $\alpha$  with respect to CoFeB thickness. Solid line is the linear fit on  $1/t_{\text{CoFeB}}$ .

layer has been reported and is attributed to spin pumping effect.<sup>17,24,25</sup> Spin pumping is a phenomena where spin current generated by the precession of magnetization in ferromagnetic layers is injected and relaxed in adjacent normal metal (NM) layer, causing an additional damping term. Depending on the relaxation time inside NM, this effect can be significant. The large enhancement of Gilbert damping has been observed in various systems with Pt capped layer.<sup>23,25</sup> Ta is known to have relative poorer spin scatter efficiency compared to Pt (spin diffusion length for Ta is about 10 nm), and hence has less pronounced spin pumping effect. The signal-to-noise ratio for our experiments, however, is sufficient to observe a clear damping increase. The linear decrease of  $\alpha$  in Fig. 5 may come from the reduced moment with decreasing thickness. It is noted that there is a slight deviation from  $1/t_{\text{CoFeB}}$  behavior at thinner film region in Fig. 5, suggesting additional origin. It is known that finite size effects in damping can exist even for layers where no spin pumping is present.<sup>26</sup> To some degree, such nonlocal background size effect in damping can be comparable to or even larger than spin pumping. The enhancement of damping in our experiment is probably due to combination of spin pumping and background size effect. Further experiments with control samples available are needed to isolate each individual contribution. Nevertheless, our result suggests that the damping constant can be tuned by varying the magnetic film thickness with the proper selection of cap layer. The intrinsic damping for our  $\text{Co}_{40}\text{Fe}_{40}\text{B}_{20}$  film is therefore only 0.004. Such small  $\alpha$  value of CoFeB, along with large TMR values is apparently advantageous for reducing spin-torque induced critical current for STT-MRAM.

#### IV. CONCLUSIONS

In summary, we have studied the magnetization dynamics of sputtered  $\text{Co}_{40}\text{Fe}_{40}\text{B}_{20}$  thin films used as FLs in MTJ stacks by broadband FMR spectrometer. We saw a strong thickness dependence of the effective magnetization and observed a large surface perpendicular anisotropy with film thickness below 2 nm. Out-of-plane angular dependence of FMR linewidth indicates large contributions from two-magnon scattering and inhomogeneous broadening for films thinner than 2 nm, and in thicker films ( $\geq 4$  nm), linewidth can be well described through the Gilbert damping. The enhanced Gilbert damping constant with reduced CoFeB thickness is probably caused by spin pumping and nonlocal background size effects.

#### ACKNOWLEDGMENTS

We acknowledge helpful discussions and editorial comments of the manuscript by Dr. R. D. McMichael and

Dr. J. W. Lau (National Institute of Standards and Technology). At Brown, the work was supported by the National Science Foundation (NSF) under Grant Nos. DMR-0907353. At Micro Magnetics, this work is funded in part by the SBIR program at National Institute of Standards and Technology and NSF IIP-0924685.

- <sup>1</sup>S. Mangin, D. Ravelosona, J. A. Katine, M. J. Carey, B. D. Terris, and E. E. Fullerton, *Nature Mater.* **5**, 210 (2006).
- <sup>2</sup>H. Yoda, T. Kishia, T. Nagasea, M. Yoshikawaa, K. Nishiyamaa, E. Kitagawaa, T. Daiboua, M. Amanoa, N. Shimomuraa, S. Takahashia, T. Kaia, M. Nakayamaa, H. Aikawaa, S. Ikegawaa, M. Nagaminea, J. Ozekia, S. Mizukamib, M. Oogane, Y. Andoc, S. Yuasad, K. Yakushijid, H. Kubotad, Y. Suzukie, Y. Nakatanif, T. Miyazakib, and K. Andod, *Current Appl. Phys.* **10**, e87 (2010).
- <sup>3</sup>V. Höink, D. Meyners, J. Schmalhorst, G. Reiss, D. Junk, D. Engel, and A. Ehresmann, *Appl. Phys. Lett.* **91**, 162505 (2007).
- <sup>4</sup>J. Wang, H. Meng, J.-P. Wang, *J. Appl. Phys.* **97**, 10D509 (2005).
- <sup>5</sup>W. H. Butler, X. G. Zhang, T. C. Schulthess, and J. M. MacLaren, *Phys. Rev. B* **63**, 054416 (2001).
- <sup>6</sup>J. Mathon and A. Umerski, *Phys. Rev. B* **63**, 220403R (2001).
- <sup>7</sup>S. Ikeda, J. Hayakawa, Y. Ashizawa, Y. M. Lee, K. Miura, H. Hasegawa, M. Tsunoda, F. Matsukura, and H. Ohno, *Appl. Phys. Lett.* **93**, 0852508 (2008).
- <sup>8</sup>L. Jiang, H. Nagauma, M. Oogane, and Y. Ando, *Appl. Phys. Expr.* **2**, 083002 (2009).
- <sup>9</sup>J. Slonczewski, *J. Magn. Magn. Mater.* **159**, L1 (1996).
- <sup>10</sup>L. Berger, *Phys. Rev. B* **54**, 9353 (1996).
- <sup>11</sup>N. Smith and P. Arnett, *Appl. Phys. Lett.* **78**, 1448 (2001).
- <sup>12</sup>S. Maat, N. Smith, M. J. Carey, and J. R. Childress, *Appl. Phys. Lett.* **93**, 103506 (2008).
- <sup>13</sup>C. Bilzer, T. Devolder, J.-V. Kim, G. Counil, C. Chappert, S. Cardoso, and P. P. Freitas, *J. Appl. Phys.* **100**, 053903 (2006).
- <sup>14</sup>S. Ikeda, K. Miura, H. Yamamoto, K. Mizunuma, H. D. Gan, M. Endo, S. Kanai, J. Hayakawa, F. Matsukura, and H. Ohno, *Nature Mater.* **9**, 721 (2010).
- <sup>15</sup>D. C. Worledge, G. Hu, D. W. Abraham, J. Z. Sun, P. L. Trouilloud, J. Nowak, S. Brown, M. C. Gaidis, E. J. O'Sullivan, and R. P. Robertazzi, *Appl. Phys. Lett.* **98**, 022501 (2011).
- <sup>16</sup>G. Malinowski, K. C. Kuiper, R. Lavrijsen, H. J. M. Swagten, and B. Koopmans, *Appl. Phys. Lett.* **94**, 102501 (2009).
- <sup>17</sup>H. Lee, L. Wen, M. Pathak, P. Janssen, P. Leclair, C. Alexander, C. K.A. Mews, and T. Mewes, *J. Phys. D: Appl. Phys.* **41**, 215001 (2008).
- <sup>18</sup>M. Oogane, T. Wakitani, S. Yakata, R. Yilgin, Y. Ando, A. Sakuma, and T. Miyazaki, *Jpn. J. Appl. Phys.* **45**, 3889 (2005).
- <sup>19</sup>D. C. Worledge and P. L. Trouilloud, *Appl. Phys. Lett.* **83**, 84 (2003).
- <sup>20</sup>M. Sparks, R. Loudon, and C. Kittel, *Phys. Rev.* **122**, 791 (1961); P. Landeros, R. E. Arias, and D. L. Mills, *Phys. Rev. B* **77**, 214405 (2008).
- <sup>21</sup>R. D. McMichael, M. D. Stiles, P. J. Chen, and W. F. Egelhoff, *J. Appl. Phys.* **83**, 7037 (1998).
- <sup>22</sup>J. Lindner, I. Barsukov, C. Raeder, C. Hassel, O. Posth, R. Meckenstock, P. Landeros, and D. L. Mills, *Phys. Rev. B* **80**, 224421(2009); H. Suhl, *Phys. Rev.* **97**, 555 (1955).
- <sup>23</sup>S. Mizukami, Y. Ando, and T. Miyazaki, *Jpn. J. Appl. Phys.* **40**, 580 (2001).
- <sup>24</sup>Y. Tserkovnyak, A. Brataas, and G. Bauer, *Phys. Rev. Lett.* **88**, 117601 (2002).
- <sup>25</sup>T. Gerrits, M. L. Schneider, and T. J. Silva, *J. Appl. Phys.* **99**, 023901 (2006).
- <sup>26</sup>A. Ghosh, J. F. Sierra, A. Auffret, U. Ebels, and W. E. Bailey, *Appl. Phys. Lett.* **98**, 052508 (2011).